ChemSearch Journal 15(1): 112 – 124, June, 2024
Publication of Chemical Society of Nigeria, Kano Chapter

Received: 02/04/2024 Accepted: 17/05/2024
http://www.ajol.info/index.php/csj

Synthesis, Characterization and *in silico* Studies of some 2-Amino-4,6-diarylpyrimidines Derived from Chalcones

***[1]Aiwonegbe, Anthony E., [1]Iyasele, Julius U. and [2]Usifoh, Cyril O.**
[1] Department of Chemistry, University of Benin, Benin City, Nigeria
[2] Department of Pharmaceutical Chemistry, University of Benin, Benin City, Nigeria
***Correspondence Email:** anthony.aiwonegbe@uniben.edu

ABSTRACT

Pyrimidine derivatives have garnered substantial research interest over the past decades. This is largely due to their wide range of biological activities as antiviral, diuretic and antitumor agents, as well as their potential therapeutic application in ameliorating several degenerative diseases. In this study, 2-amino-4,6-diarylpyrimidines were synthesized from their respective 1,3-diphenylprop-2-en-1-one (chalcone) precursors. The chalcones were condensed with guanidine carbonate by refluxing in dimethylformamide for 4 hours at 160˚C to obtain the following compounds: 4,6-diphenyl-pyrimidin-2-ylamine (PAA_1), 4-(4-nitro-phenyl)-6-phenylpyrimidin-2-ylamine (PAA_2), 4-phenyl-6-(3,4,5-trimethoxy-phenyl)pyrimidin-2-ylamine (PAA_3) and 4-phenyl-6-(3,4,5-trimethoxy-phenyl)pyrimidin-2-ylamine (PAA_4). TLC analysis was used to monitor the purity of the synthesized compounds, and their melting points were determined using the open capillary method with a Kofler Electrothermal melting point apparatus. They were characterized using IR, ^{1}H-NMR, ^{13}C-NMR and GC - MS. The biological activities of the title compounds were predicted using the Gaussian 16 software suite-36 (for full geometry optimization in chloroform and gas phase) and the SwissADME web tool for lipophilicity and hydrophilicity. The compounds were obtained in good yield, and the characteristic N-H stretch of the $-NH_2$ group (free and H-bonded) was observed at 3503, 3380 cm^{-1}(PAA_1); 3492, 3317 cm^{-1}(PAA_2); 3194, 3309 cm^{-1} (PAA_3); and 3466, 3313 cm^{-1}(PAA_4). The amino protons showed a broad peak between 4.47 – 5.31 ppm while the characteristic C2 and C5 of 2-aminopyrimidines resonated at 105.34 and 163.03 ppm respectively. The logP values revealed that the lipophilicity of the compounds decreased in the order: PAA_1< PAA_2< PAA_3< PAA_4. The computations on the optimized geometry established the possible application of the compounds in the synthesis of modern pharmaceuticals.

Keywords: Chalcone, Characterization, Computation, Optimized geometry, Pyrimidine

INTRODUCTION

Heterocyclic compounds are found in nature, and several of them are involved in biological processes (Al-Mulla, 2017). Nitrogen-containing heterocyclic compounds, most of which are weak bases generally known as alkaloids, are commonly found in plants. Heterocycles possess intrinsic reactivity. This makes it easy for them to undergo versatile and productive transformations (Isambert and Lavilla, 2008).

Most of these reactions and their products have large scale uses in drug and dye companies (Remington, 2005).

Pyrimidine is an aromatic organic heterocyclic compound and its derivatives have well known age-long therapeutic applications (Kumar *et al*., 2018). One of the major reasons for their broad-spectrum pharmacological properties is the presence of a pyrimidine nucleus in the structure of the nucleotide bases, and these bases make up the molecular structures of DNA (deoxyribonucleic acid) and RNA (ribonucleic acid) (Lagoja, 2005). Pyrimidines are synthesized from chalcones mainly through condensation reactions (Ebraheem, 2013). For example, thiourea reacts with chalcones in the presence of NaOH to produce 4,6-disubstituted pyrimidine-2-yl thiol derivatives (Azam *et al*., 2008), and guanidine hydrochloride condenses with chalcones in the presence of NaOH to form 2- amino-4,6-disubstituted pyrimidines (Udupi *et al*., 2005) and substituted pyrimidin-2(1*H*)-ones have been synthesized from chalcones (Ajani *et al*., 2011).

In therapeutics, drug resistance is a major concern (Ayukekbong *et al*., 2017). Disease-causing organisms are developing new resistance mechanisms (Andrews and Ahmed, 2015). This has become a threat to the ability to treat common infectious diseases (WHO, 2021). It is therefore imperative to continuously explore new compounds as potential drug candidates, and in this exploration, researchers have been investigating heterocycles containing pyrimidine moieties (Kumar *et al*., 2018, Rao *et al*., 2012, Vachala et al., 2012). It has been established that 2-aminopyrimidine is one of the vital

pharmacophores responsible for the biological activities of pyrimidine and its derivatives (Koroleva., 2010).

In view of the above and our interest in studying novel drugs, we wish to report the synthesis and characterization of four different compounds of 2-amino-4,6-diarylpyrimidines. We also investigated these compounds, *in silico*, as potential drugs.

MATERIALS AND METHODS

All the chemicals used in this study were of analytical grade and were used without further purification. The chalcones were used as synthesized and characterized by Aiwonegbe and Iyasele (2022). Guanidine carbonate powder (99%) and dimethylformamide (99.9%) were obtained from BDH Chemicals Ltd., Poole, England. Ethanol, methanol, n-hexane, and ethyl acetate were obtained from JHD Chemicals, Guangdong, China.

Thin layer chromatography was carried out using analytical TLC plates precoated with silica gel 60 F_{254}, 20 cm ×20 cm (Merck KGaA, Darmstadt, Germany) and visualized under a UV lamp. Fluorescent compounds were visualized at 366 nm, while nonfluorescent compounds were visualized at 254 nm. Melting points were determined with a Kofler Electrothermal melting point apparatus (CAT No 1A6304, England) in open capillary tubes and were uncorrected.

The IR spectra were recorded using KBr discs on a Spectrum Two DTGS Instrument No. L16004001 running on Perkin Elremer (Liantrisant, UK). 1H and 13C-NMR data were recorded on a Varian Gemini 400 (400 MHz) (Varian Inc., Pal Alto, California, USA), while the chemical shifts are reported in ppm relative to tetramethylsilane (TMS) as the internal reference standard. The multiplicities are represented as follows: s = singlet, d = doublet, t = triplet, q = quartet and m = multiplet

Synthesis of 2-aminopyrimidines

The general method used for the synthesis of the 2-amino pyrimidine derivatives is shown in Scheme 1.

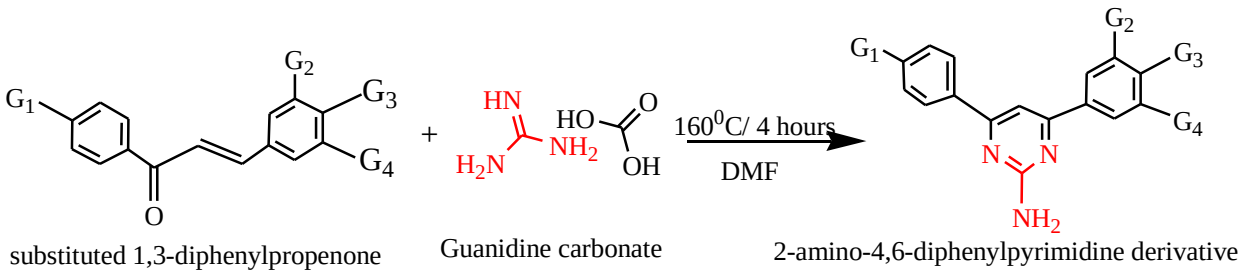

PAA1 : $G_1 = G_2 = G_3 = G_4 = H$ **PAA3** : $G_1 = H$, $G_2 = G_3 = G_4 = OCH_3$

PAA2 : $G_1 = NO_2$, $G_2 = G_3 = G_4 = H$ **PAA4** : $G_1 = NO_2$, $G_2 = G_3 = G_4 = OCH_3$

Scheme 1: General reaction scheme

The method described by Sharma and Sharma, (2011) was adopted for the synthesis of the 2-aminopyrimidine derivatives. Some modifications were made by pre-drying the DMF used as the solvent, increasing the reflux time by one hour, using and oil bath for heating and allowing the reaction mixture to stand for 24 hours before filtration.

Synthesis of 4,6-diphenylpyrimidin-2-ylamine (PAA1)

To a 100 mL round bottom flask, 1 g (4.8 mmol) of 1,3-diphenylprop-2-en-1-one and 0.86 g (4.8 mmol) of guanidine carbonate were added. The reactants were thoroughly mixed together and dissolved in 60 mL of dimethylformamide (DMF), which was previously dried with KOH pellets for 72 hours. It was then heated for 4 hours at 160°C using an oil bath after which it was cooled to room temperature and poured into crushed ice. The cooled mixture was allowed to stand for 24 hours after which it was filtered and the filtrate was washed with distilled water. The purity of the product was monitored using TLC. The product was air-dried at room temperature. The yield was calculated and the melting point was determined.

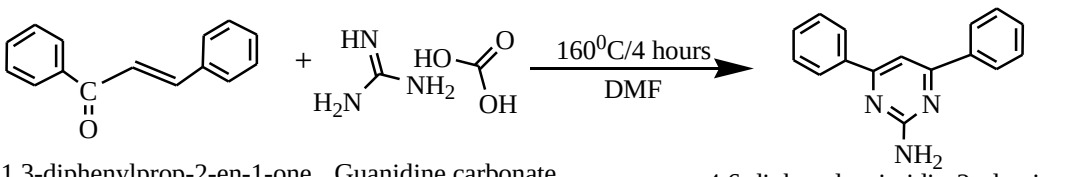

Synthesis of 4-(4-nitro-phenyl)-6-phenylpyrimidin-2-ylamine (PAA2)

To a 100 mL round bottom flask, 1 g (4 mmol) of 1-(4-nitrophenyl)- 3-phenylprop-2-en-1-one and 0.72 g (4 mmol) of guanidine carbonate were added. The procedure described in (***PAA1)*** above was adopted.

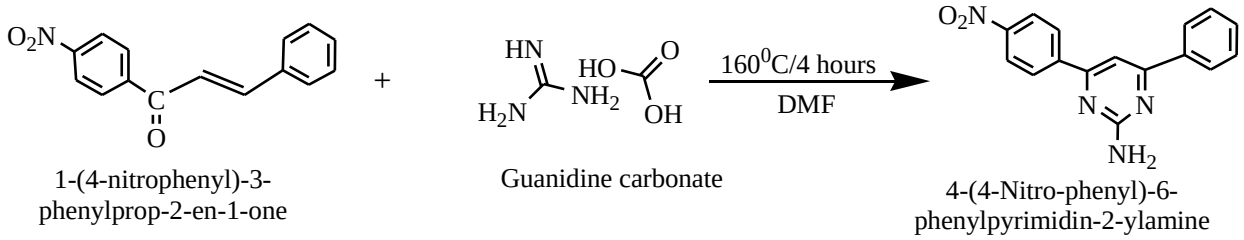

1-(4-nitrophenyl)-3-phenylprop-2-en-1-one Guanidine carbonate 4-(4-Nitro-phenyl)-6-phenylpyrimidin-2-ylamine

Synthesis of 4-phenyl-6-(3,4,5-trimethoxy-phenyl)pyrimidin-2-ylamine (PAA3)

To a 100 mL round bottom flask, 1 g (3.4 mmol) of 1-phenyl-3-(3,4,5-trimethoxyphenyl) prop-2-en-1-one and 0.61 g (3.4 mmol) of guanidine carbonate were added The procedure described in (***PAA1)*** above was adopted.

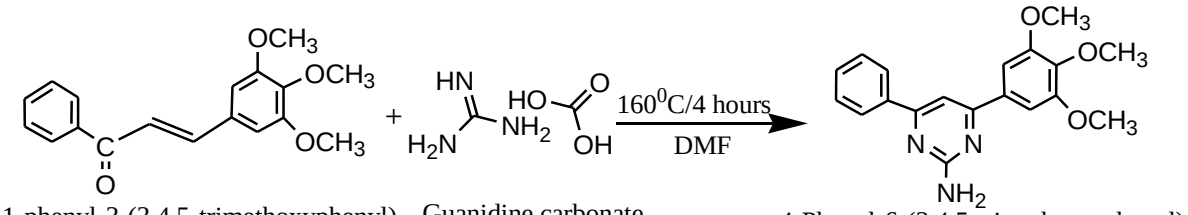

1-phenyl-3-(3,4,5-trimethoxyphenyl) prop-2-en-1-one Guanidine carbonate 4-Phenyl-6-(3,4,5-trimethoxy-phenyl) pyrimidin-2-ylamine

Synthesis of 4-(4-nitro-phenyl)-6-(3,4,5-trimethoxyphenyl)pyrimidin-2-ylamine (PAA4)

To a 100 mL round bottom flask, 1 g (2.9 mmol) of 1-(4-nitrophenyl)-3-(3,4,5-trimethoxyphenyl)prop-2-en-1-one and 0.52 g (2.9 mmol) of guanidine carbonate were added. The procedure described in (***PAA1)*** above was adopted.

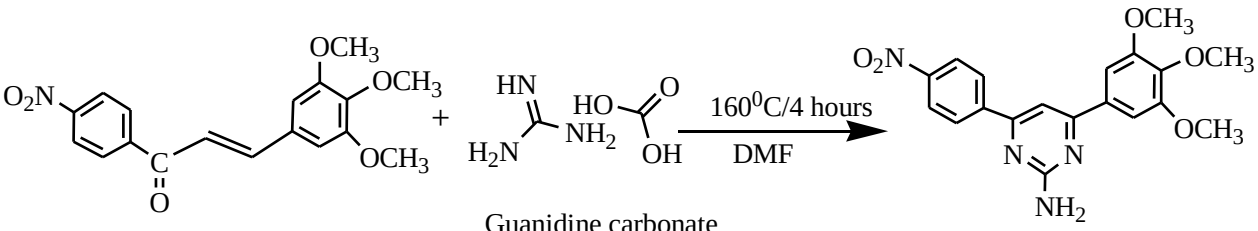

1-(4-nitrophenyl)-3-(3,4,5-trimethoxyphenyl) prop-2-en-1-one Guanidine carbonate 4-(4-nitro-phenyl)-6-(3,4,5-trimethoxy phenyl)pyrimidin-2-ylamine

Computational methods

All quantum chemical computations were carried out within the Gaussian 16 software suite running on SEAGrid, DFT methods are known to give a reliable description of the geometry, vibrational spectra and molecular orbital calculations for organic compounds (Chugunova *et al*, 2022, Umar *et al*., 2021, Korkmaz *et al*., 2023, Sudha *et al*., 2022). Gaussian 16 software was used to carry out full geometry optimization in the gas phase and chloroform (solvent). Harmonic vibrational frequency calculations of PAA_1, PAA_2, PAA_3 and PAA_4 were performed using DFT with the Becke-3-Lee-Yang-Parr (B3LYP) functional (Kanagathara, *et al*., 2022, Mennucci *et al*., 2022). The standard 6-311++G basic set was used for all the atoms. Computations in chloroform were carried out based on the polarizable continuum model (PCM) (Matsuzawa *et al*., 2001, Jamroz, 2004). The VEDA4 program (Darugar *et al*., 2021) was used to determine the normal vibrational modes based on the potential energy distribution (PED) Gauss-View program (Frisch *et al*., 2000), which was also used for visual verification of the vibrational mode assignments obtained from VEDA4. The optimized structures of the four compounds were used for computing chemical shifts with the Gauge-Including Atomic Orbital method (Gauss, 1992) and TMS was used as the reference. The HOMO (E_{HOMO}) and LUMO

(E_{LUMO}) energy values were used to calculate global chemical reactivity descriptors such as ionization potential ($I = -E_{HOMO}$), electron affinity ($A= -E_{LUMO}$), (Ayalew, 2022) electronegativity ($\chi = (1+A)/2$), chemical hardness ($\eta = (1 - A)/2$), chemical softness ($S = 1/2\eta$), chemical potential ($\mu = - (1 + A)/2$), and electrophilicity index ($\omega = \mu^2/2\eta$) (Umar and .Abdalla, 2017). The SwissADME web tool was used to predict drug-related parameters namely lipophilicity and hydrophilicity (Mennucci *et al*., 2010).

Results and Discussion

Physical Characteristics

The physical characteristics of the synthesized 2-aminopyrimidines are shown in Table 1 below. The melting point range of the synthesized compounds shows that they are relatively pure. However, PAA1 and PAA3 were slightly out of range (above 2^0C) which might be due to lack of crystallinity (Hart *et al.*, 2012).

Table 1: Physical characteristics of the synthesized 2-aminopyrimidine derivatives

Compound ID	Mol. mass	Mol. formular	Rf	Solvent	Colour
PAA1	247.29	$C_{16}H_{13}N_3$	0.94	D, DC, P	Bright yellow
PAA2	292.10	$C_{16}H_{12}N_4O_2$	0.97	D, DC, P	Reddish brown
PAA3	337.14	$C_{19}H_{19}N_3O_3$	0.83	D, DC, P	Orange
PAA4	382.13	$C_{19}H_{18}N_4O_5$	0.83	D, DC, P	Milky

TLC solvent system: n-hexane/ethylacetate (1:2)
KEY: Rf = Retention factor; D = DMSO; DC = dichloromethane; P = pyridine

Spectroscopic Data

4,6-diphenylpyrimidin-2-ylamine (PAA1)

Yield 33.74%, m.p. 116-120°C, IR (KBr, cm^{-1}): 3503, 3380 (-NH_2 free and H-bonded), 1669 (C=N), 1513 (=C=C=), 2937 (C-H stretch), 998, 812 (ring breathing mode).

GC and mass spectrometry revealed an M^+H peak at 248 (18%), an M^+-H peak at 246 (72%) and an M^+ peak at 247 (100%), which is equivalent to the molecular weight of the compound.

^{1}H NMR (400 MHz, $CDCl_3$, ppm): 7.66 - 7.33 (10H, m, Ar-*H*), 5.51 (1H, s, -C*H* pyrimidine), 4.10 (2H, s, -NH_2 pyrimidine).

^{13}C NMR (100 MHz, $CDCl_3$, ppm): 167.04 (2C, N-*C* pyrimidine), 164.15 (1C, N-*C*=N pyrimidine), 138.30 (2C, Ar-*C*), 129.99 (2C, Ar-*C*), 129.75 (4C, Ar-*C*), 129.35 (4C, Ar-*C*), 105.18 (1C, *C*-pyrimidine).

4-(4-nitrophenyl)-6-phenylpyrimidin-2-ylamine (PAA2)

Yield 72.77%, m.p. 198-200°C, IR (KBr, cm^{-1}): 3492, 3317, 3198 (-NH_2 free and H-bonded), 1625 (C=N), 1585 (=C=C=), 2117 (C-H stretch), 1013, 823 (ring breathing mode).

GC and mass spectrometry revealed an M^+H peak at 293 (19%), an M^+-H peak at 291 (25%) and an M^+ peak at 292 (100%), which is equivalent to the molecular weight of the compound.

^{13}C NMR (100 MHz, $CDCl_3$, ppm): 165.66 (1C, *C*=N pyrimidine), 164.09 (1C, N-*C*=N pyrimidine), 153.67 (1C, *C*=N pyrimidine), 148.99 - 128.39 (12C, Ar-*C*), 102.75 (1C, *C*- pyrimidine).

4-phenyl-6-(3,4,5-trimethoxyphenyl)pyrimidin-2-ylamine (PAA3)

Yield 11.34%, m.p. 80-86°C, IR (KBr, cm^{-1}): 3194, 3309, 3440 (-NH_2 free and H-bonded), 1632 (C=N), 1572 (=C=C=), 2937 (C-H stretch), 998, 827 (ring breathing mode).

GC and mass spectrometry revealed an M^+H peak at 338 (22%), an M^+-H peak at 336 (13%) and an M^+ peak at 337 (100%), which is equivalent to the molecular weight of the compound.

^{1}H NMR (400 MHz, $CDCl_3$, ppm): 8.14 (2H,d, -C-*H* pyrimidine), 7.58 (1 H, m, - Ar-*H*), 7.50 (1H, t, Ar-*H*). 6.89(1H, s, -C-*H* pyrimidine). 6.49 (2H, s, Ar-*H*), 5.20 (2H, s, C -NH_2 pyrimidine), 4.14 - 3.93 (6H, s, 3H, s, alkoxy-*H*).

^{13}C NMR (100 MHz, $CDCl_3$, ppm): 158.70 (1C, N-*C*=N pyrimidine), 155.50 (1C, N-*C*=N pyrimidine), 153.71 (1C, -N-*C* pyrimidine), 149.10 (2C, Ar-*C*), 136.50 (1C, Ar-*C*), 133.50 (1C, Ar-*C*), 129.16 (1C, Ar-*C*), 129.05 (2C, Ar-*C*), 128.16 (1C, Ar-*C*), 127.57 (2C, Ar-*C*), 106.61 (1C, *C*-pyrimidine), 103.63 (2C, Ar-*C*), 61.06 (1C,alkoxy-*C*), 56.60, 56.24 (2C, alkoxy-*C*).

4-(4-nitrophenyl)-6-(3,4,5-trimethoxyphenyl)pyrimidin-2-ylamine (PAA4)

Yield 77.63%, m.p. 188-190°C, IR (KBr, cm^{-1}): 3466, 3313 (-NH_2 free and H-bonded), 1684 (C=N), 1572 (=C=C=), 3026 (C-H stretch), 1028, 842 (ring breathing mode).

GC and mass spectrometry revealed an M^+H peak at 383 (22%), an M^+-H peak at 381 (8%) and an M^+ peak at 382 (100%), which is equivalent to the molecular weight of the compound.

^{1}H NMR (400 MHz, $CDCl_3$, ppm): 8.27 (2H, d, Ar-*H*), 7.83 (2H, d, Ar-*H*), 6.38 (1H, s, Ar-*H*), 6.51 (2H, s, Ar-*H*), 5.31 (2H, s, -NH_2 pyrimidine), 4.01 - 3.72 (6H, s, 3H, s, alkoxy-*H*)

^{13}C NMR (100 MHz, $CDCl_3$, ppm): 169.70 (1C, H_2N-*C*=N pyrimidine), 167.50 (1C, -*C*=N

pyrimidine), 164.30 (1C, -*C*=N pyrimidine), 154.46 (O_2N-*C*-Ar 147.60), 149.10 (2C, Ar-*C*), 142.60 (1C, Ar-*C*), 133.20 (1C, Ar-*C*), 130.80 (1C, Ar-*C*), 129.00 (2C, Ar-*C*), 124.35 (2C, Ar-*C*), 108.40 (1C, *C*-pyrimidine), 105.44 (2C, Ar-*C*), 61.91 (1C,alkoxy-*C*), 57.30 (2C, alkoxy-*C*).

Computational results

The computed NMR of the synthesized compounds (PAA1, PAA2, PAA3 and PAA4) is provided in detail in Tables SI**A** (a) - SI**A** (d). The reactivity descriptors are shown in Table SI**B**. The lipophilicity and hydrophilicity of the title compounds were estimated using SWISS-ADME and are shown in Table SI**C**. Other physicochemical properties, pharmacokinetics, drug-likeness and medicinal chemistry aspects of the compounds are displayed in a one-panel output form in Figures SI**C** (a) - SI**C** (d). The coordinates of the optimized compounds in the gas phase and in the solvent (chloroform) were also computed alongside the complete IR analysis of the four compounds, using VEDA resulting in the optimized geometry of the compounds as shown in Figures SIA (a) – SIA (d).

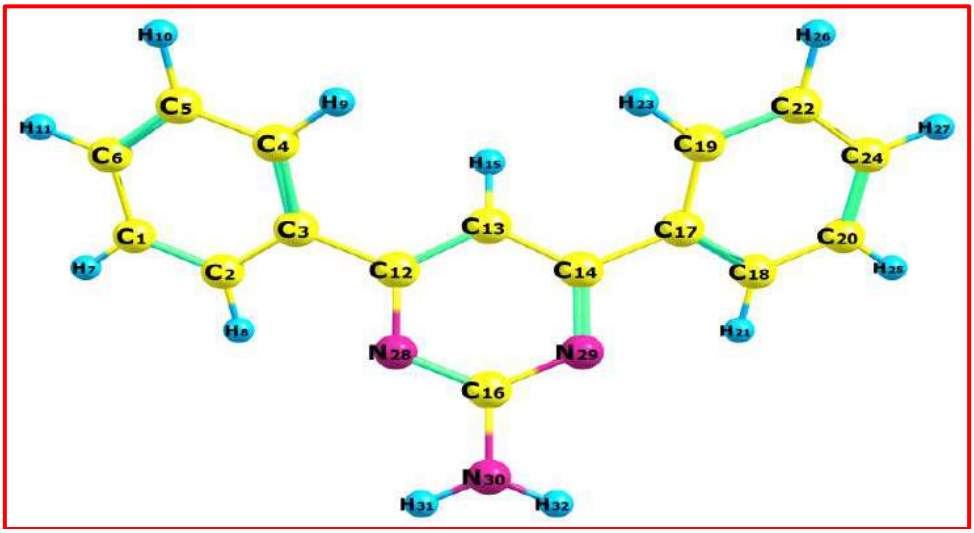

Figure SIA (a): Optimized geometry of PAA1 for atom labeling

Table SIA (a): Computed chemical shifts of ^{1}H and ^{13}C (ppm) for PAA1

	δ ^{1}H (ppm)			δ ^{13}C (ppm)	
Atom labeling	Experimental data	Computed data	Atom labeling	Experimental data	Computed data
7	7.58	8.49	1	130.00	152.27
8	8.09	9.29	2	129.75	151.00
9	7.66	8.97	3	138.31	162.43
10	7.52	8.44	4	128.96	149.99
11	7.30	8.52	5	129.89	151.63
15	5.51	8.28	6	131.58	154.44
21	8.09	9.29	12	164.16	191.60
23	7.66	8.97	13	105.18	122.64
25	7.58	8.49	14	164.16	191.60
26	7.52	8.44	16	167.04	183.88
27	7.30	8.52	17	138.31	162.43
31	3.37	5.31	18	129.75	151.00
32	3.37	5.31	19	128.96	149.99
			20	130.00	152.27
			22	129.89	151.63
			24	131.58	154.44

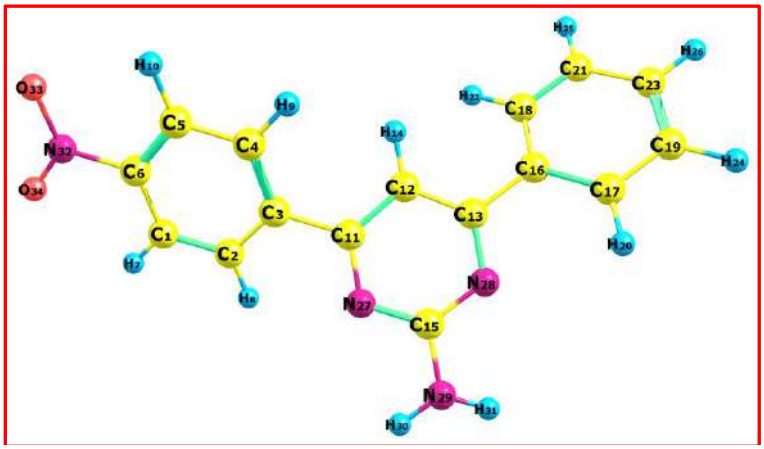

Figure SIA (b): Optimized geometry of PAA2 for atom labeling

Table SI**A** (b): Computed chemical shifts of ^{1}H and ^{13}C (ppm) for PAA2

	δ ^{1}H (ppm)			δ ^{13}C (ppm)	
Atom labeling	Experimental data	Computed data	Atom labeling	Experimental data	Computed data
7	8.69	9.42	1	127.55	146.14
8	8.28	9.33	2	131.19	151.50
9	8.17	8.93	3	151.82	170.95
10	8.69	9.31	4	128.97	150.41
14	7.34	8.31	5	123.42	145.77
20	7.92	9.32	6	153.46	171.21
22	7.90	8.91	11	164.09	189.07
24	7.74	8.43	12	103.23	123.41
25	7.76	8.47	13	164.32	192.64
26	7.66	8.50	15	163.03	183.61
30	4.44	5.36	16	143.91	161.80
31	4.44	5.40	17	131.05	151.39
			18	128.39	150.08
			19	137.71	152.27
			21	137.05	151.69
			23	140.65	154.78

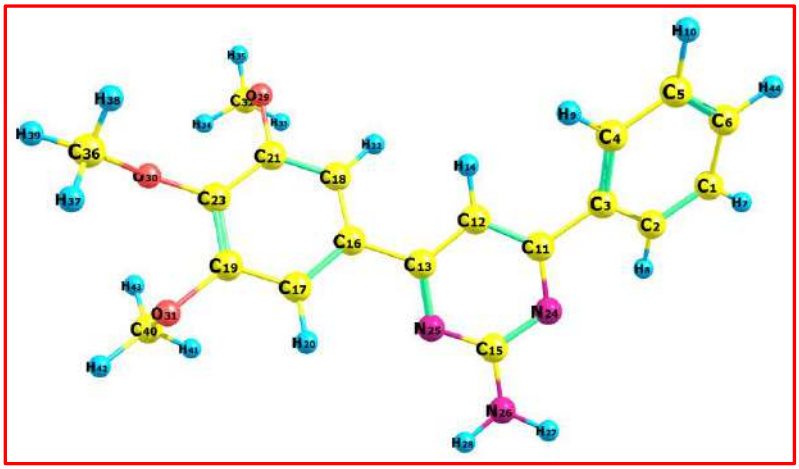

Figure SIA(c): Optimized geometry of PAA3 for atom labeling

Table SIA (c): Computed chemical shifts of ^{1}H and ^{13}C (ppm) for PAA3

	δ ^{1}H (ppm)			δ ^{13}C (ppm)	
Atom labeling	Experimental data	Computed data	Atom labeling	Experimental data	Computed data
7	8.11	8.46	1	104.97	152.24
8	8.14	9.34	2	103.63	151.18
9	8.14	8.87	3	128.16	162.12
10	8.11	8.43	4	103.63	149.74
14	7.52	8.25	5	104.97	151.51
20	8.12	8.77	6	106.61	154.42
22	8.05	8.30	11	153.71	191.69
27	6.49	5.25	12	77.34	122.09
28	6.49	5.25	13	129.05	189.83
33	6.23	3.42	15	152.72	183.62
34	6.23	4.43	16	105.12	158.31
35	6.23	3.97	17	77.02	139.66
37	5.20	4.07	18	76.70	138.86
38	5.20	3.60	19	129.11	178.27
39	5.20	4.14	21	129.05	177.31
41	6.23	3.56	23	127.57	171.61
42	6.23	4.08	32	56.24	65.30
43	6.23	4.32	36	61.06	64.54
44	7.57	8.47	40	56.60	64.89

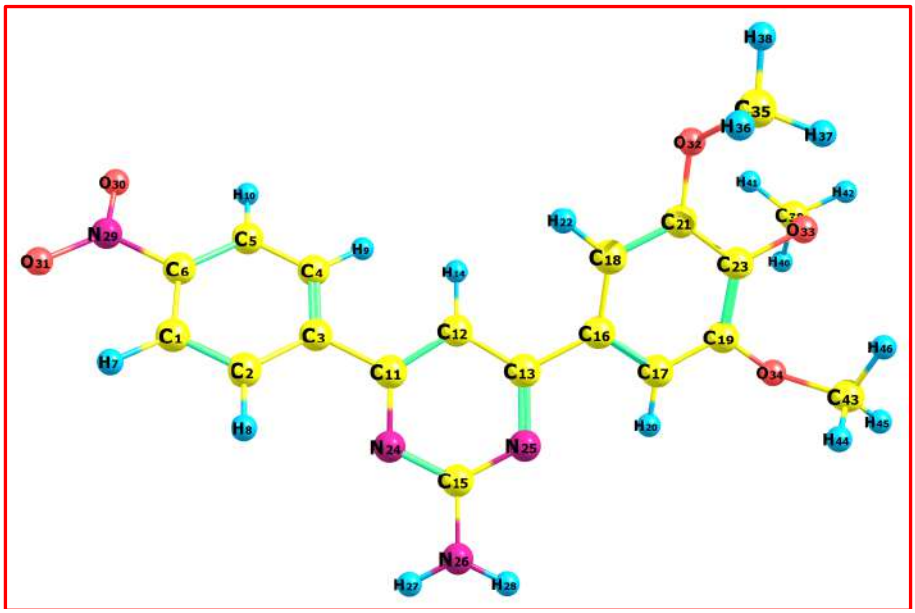

Figure SIA (d): Optimized geometry of PAA4 for atom labeling

Table SIA (d): Computed chemical shifts of ^{1}H and ^{13}C (ppm) for PAA4

	δ ^{1}H (ppm)			δ ^{13}C (ppm)	
Atom labelling	Experimental data	Computed data	Atom labelling	Experimental data	Computed data
7	8.35	9.28	1	74.22	146.23
8	8.13	9.47	2	74.51	152.36
9	8.05	8.90	3	77.43	171.27
10	8.38	9.30	4	74.51	150.45
14	7.44	8.19	5	74.22	145.83
20	7.33	8.75	6	77.93	170.93
22	7.29	8.27	11	129.00	189.26
27	5.31	5.35	12	105.44	122.81
28	5.31	5.39	13	154.46	190.96
36	3.71	3.46	15	124.85	183.65
37	4.00	4.41	16	76.82	157.66
38	3.95	4.00	17	73.51	139.89
40	3.85	4.03	18	73.51	138.94
41	3.85	3.63	19	78.44	178.04
42	3.85	4.20	21	78.44	177.17
44	3.72	3.54	23	77.43	171.98
45	3.88	4.11	35	57.30	65.52
46	4.00	4.37	39	61.92	64.58
			43	57.30	65.05

Table SIB: Reactivity descriptors of PAA1, PAA2, PAA3 and PAA4

Descriptors	PAA1	PAA2	PAA3	PAA4
HOMO (eV)	-7.61	-7.99	-7.54	-7.86
LUMO (eV)	-0.97	-1.97	-0.98	-1.94
HOMO-LUMO Gap (eV)	6.63	6.02	6.56	5.92
Ionization potential (eV)	7.61	7.99	7.54	7.86
Electron affinity (eV)	0.97	1.97	0.98	1.94
Chemical potential (eV)	4.29	4.98	4.26	4.90
Electronegativity (eV)	-4.29	-4.98	-4.26	-4.90
Global hardness (eV)	3.32	3.01	3.28	2.96
Global softness (eV^{-1})	0.15	0.17	0.15	0.17
Electrophilicity index (eV)	2.77	4.11	2.76	4.06

Table SI**C**: Estimated lipophilicity and hydrophilicity using SWISS-ADME

Compound Label	Structure	Lipophilicity ($log_{PO/W}$)	Hydrophilicity [log S(ESol)]
PAA1	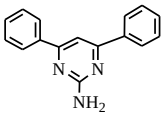	2.98	-3.95
PAA2	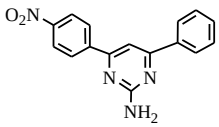	2.89	-4.08
PAA3	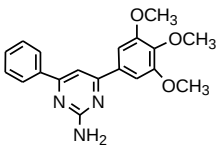	2.19	-3.96
PAA4	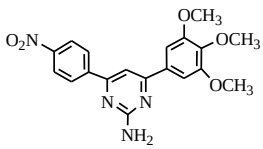	2.17	-4.13

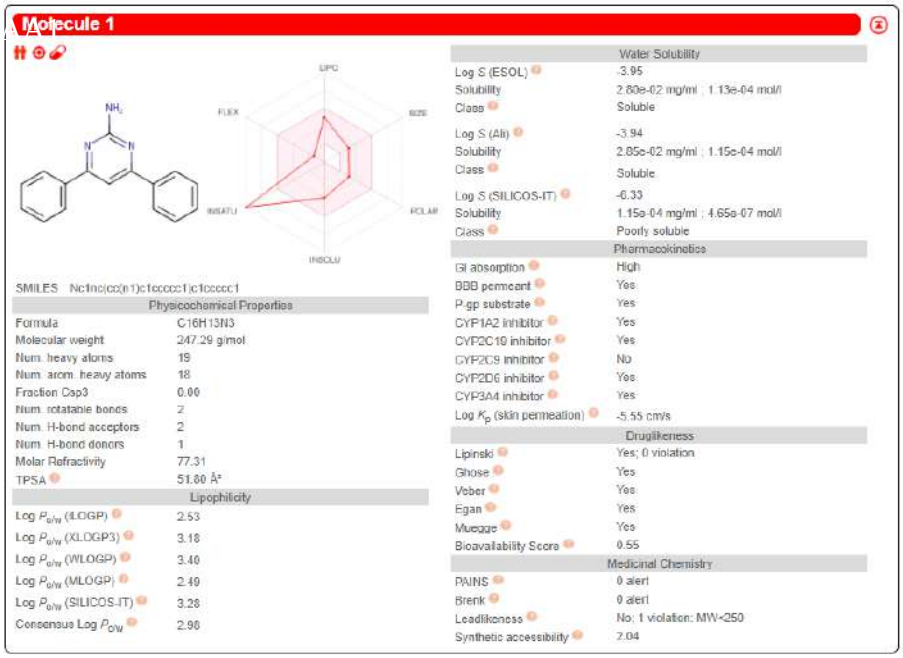

Figure SIC (a): One-panel -per-molecule output for the computed values of PAA1

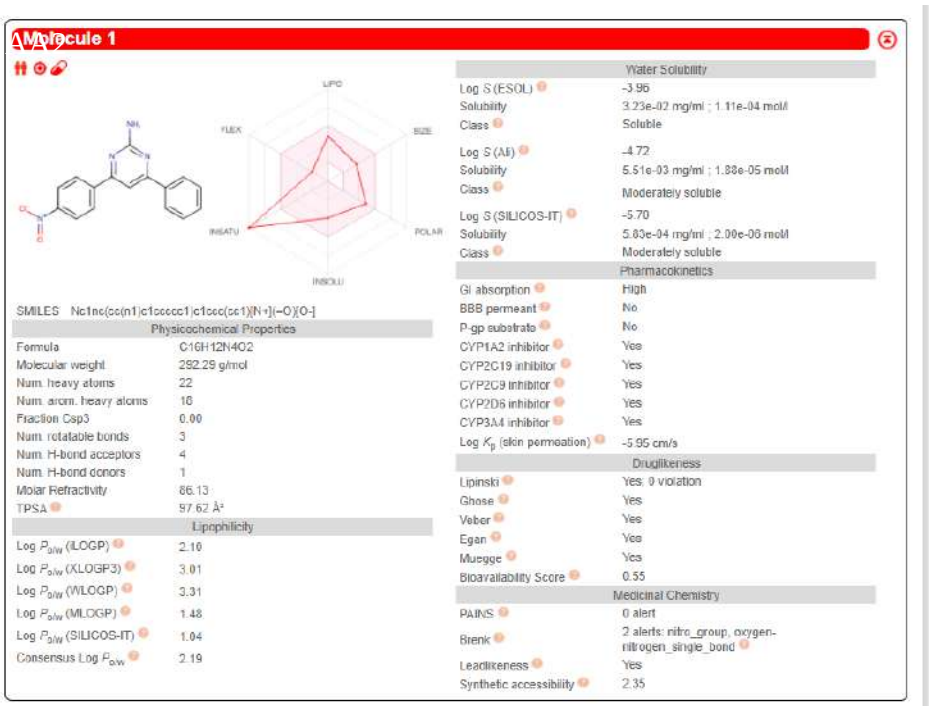

Figure SIC (b): One-panel-per-molecule output for the computed values of PAA2

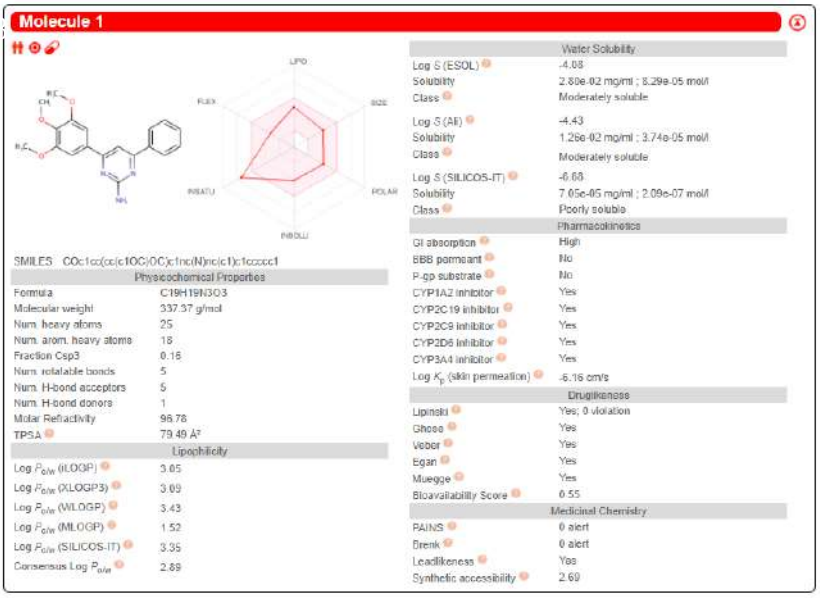

Figure SIC (c): One-panel-per-molecule output for the computed values of PAA3

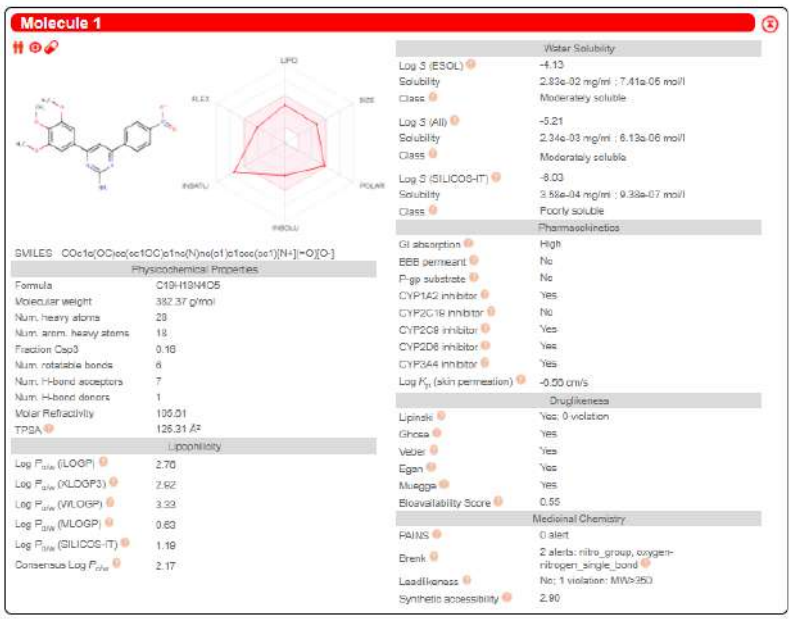

Figure SIC (d): One-panel-per-molecule output for the computed values of PAA4

DISCUSSION

The lipophilicity of compounds plays a crucial role in determining their physicochemical and biological properties (Pallicer *et al*., 2014). LogPO/W, a commonly used measure of lipophilicity, reflects the ability of a compound to partition between hydrophobic and hydrophilic phases. Optimal LogPO/W values are particularly desirable in the context of drug development because they can influence a compound's absorption, distribution, metabolism, and excretion (ADME) properties.

In this study, we assessed the lipophilicity of four compounds, namely PAA1, PAA2, PAA3, and PAA4. All of these compounds exhibited lipophilic characteristics, with LogP values greater than 0 or P values exceeding 1. Among the compounds, PAA4 displayed the highest lipophilicity, as evidenced by its lowest LogP value of 2.17. This finding suggests that PAA4 has a greater affinity for hydrophobic environments than the other compounds investigated (Anaridha *et al*., 2021).

Furthermore, the derivatization of PAA1 led to a significant increase in its lipophilicity. This is evidenced by the lower LogP values observed for PAA2, PAA3, and PAA4 in comparison to those of PAA1. Derivatization is a common strategy employed in drug development to enhance the pharmacokinetic properties of compounds,

including their lipophilicity. The observed increase in lipophilicity following derivatization underscores the potential utility of this approach in modulating the ADME profile of compounds intended for therapeutic applications (Waring, 2010; Arnott and Planey, 2012).

Overall, the lipophilicity profiles of the compounds investigated in this study provide valuable insights into their potential suitability as drug candidates. Further investigations into the relationship between lipophilicity and other pharmacological properties are warranted to fully elucidate the therapeutic potential of these compounds. Additionally, exploring strategies to optimize the lipophilicity of compounds could enhance their efficacy and safety profiles in clinical settings.

CONCLUSION

The synthesis, characterization, and computational analysis of four 2-amino-4,6-diarylpyrimidine derivatives have provided valuable insights into the potential pharmacological applications of pyrimidine-based compounds. Pyrimidine, as a fundamental component of DNA and RNA, exhibits significant synthetic versatility and serves as a crucial intermediate in the formulation of various biologically active compounds.

Our study underscores the importance of exploring pyrimidine derivatives as potential candidates for drug development. The versatility of pyrimidine as a synthon and intermediate offers promising opportunities for the synthesis of novel compounds with diverse biological activities. By synthesizing and characterizing these derivatives, we have contributed to the growing body of knowledge regarding the structural and pharmacological properties of pyrimidine-based molecules.

Moreover, our computational analyses have provided valuable insights into the structural features and molecular interactions of the synthesized derivatives, further facilitating their potential application in drug design and development.

Furthermore, the insights gained from this study highlight the potential of pyrimidine scaffolds in addressing the global health challenge of drug resistance. As drug resistance continues to pose a significant threat to public health, the development of new drugs and pharmaceutical formulations is crucial. Pyrimidine derivatives offer a promising avenue for the discovery of novel therapeutics that can overcome drug resistance mechanisms and improve treatment outcomes.

This research contributes to the understanding of pyrimidine chemistry and its implications for drug discovery. By elucidating the structure-activity relationships of pyrimidine derivatives, we pave the way for the development of innovative drugs and therapeutic strategies to address unmet medical needs and combat drug resistance. However, further investigations into the pharmacological properties and therapeutic potential of pyrimidine-based compounds are warranted to fully understand their clinical utility and impact on global health.

ACKNOWLEDGMENTS

The authors are grateful to Professor Ramasami Ponnadurai and Lydia Rhyman of the Computational Chemistry Group, Department of Chemistry, Faculty of Science, University of Mauritius, Reduit, Mauritius for providing the computational data for this research.

Special appreciation also goes to Dr. Peter Dziemba of the Institut für Pharmazeutische und Medizinische Chemie, Corrensstraße, Germany who ran the mass spectrum for our compounds and Frau Martina Hense, of the Department of Pharmaceutical Chemistry, University of Jena, Philosophenweg, Jena, Germany for providing the ^{1}H-NMR and ^{13}C-NMR spectra.

REFERENCES

Aiwonegbe, A. E. and Iyasele J.U. (2022): Synthesis, characterization and insect repellant activity of some chalcone derivatives. *Journal of Chemical Society of Nigeria*, 47(1): 018 - 028 .

Ajani, O.O., Ituen, R.I. and Falomo A. (2011): Facile synthesis and characterization of substituted pyrimidin-2(1*H*)-ones and their chalcone precursors. *Pakistan Journal of Science and Industrial Research*, 54:59-67. https://doi.org/10.52763/PJSIR.PHYS.SCI.54.2011.59.67

Al-Mulla, A. (2017): A Biological importance of heterocyclic compounds. *Der Pharma Chemica*, 9(13):141-147.

Anaridha, S., Imran, P.K.M., Meeran, I.S. and Shabeer, T.K. (2021): comparative theoretical analysis using DFT & MP2 calculations, ADMET profiling and docking studies of the drug telotristat ethyl. *Journal of the Indian Chemical Society*, 98(12): 100248. https://doi.org/10.1016/j.jics.2021.100248

Andrews, B. and Ahmed, M. (2015): An efficient synthesis, characterization and anti-bacterial activity of pyrimidine bearing 1,3,4-thiadiazole derivatives. *Indian J. Chem*, 54:406-411.

Arnott, J. and Planey, S. (2012): The influence of lipophilicity in drug discovery and design. Expert Opinion on Drug Discovery, 7:863 - 875. https://doi.org/10.1517/17460441.2012.714363

Ayalew, M.E. (2022): DFT Studies on molecular structure, thermodynamics parameters, HOMO-LUMO and spectral analysis of

pharmaceuticals compound quinoline (benzo[b]pyridine). *Journal of Biophysical Chemistry*, 13:29-42. https://doi.org/10.4236/jbpc.2022.133003

Ayukekbong, J.A., Ntemgwa, M. and Atabe, A.N. (2017): The threat of antimicrobial resistance in developing countries: causes and control strategies. *Antimicrob. Resists. Infect. Control*, 6:4. https://doi.org/10.1186/s13756-017-0208-x

Azam, M.A., Kumar, B.R., Shalini, S., Suresh, B. and Reddy, T.K. (2008): Synthesis and biological screening of 5-{[(4,6-Disubstituted pyrimidine-2-yl)thio]methyl}-N-phenyl-1,3,4-thiadiazol-2-amines. *Indian Journal of Pharmaceutical Sciences*, 70(5):672-7. https://doi.org/10.4103/0250-474X.45416. PMID: 21394274; PMCID: PMC3038302.

Chugunova, E., Shaekhov, T., Khamatgalimov, A., Gorshkov, V. and Burilov, A. (2022): DFT quantum-chemical calculation of thermodynamic parameters and DSC measurement of thermostability of novel benzofuroxan derivatives containing triazidoisobutyl fragments. *Int. J. Mol. Sci.* 23(3):1471. https://doi.org/10.3390/ijms23031471. PMID: 35163391

Darugar, V., Mohammad, V., Sayyed, F.T., Fadhil, S.K. (2021): Validation of Potential Energy Distribution by VEDA in vibrational assignment some of β-diketones; comparison of theoretical predictions and experimental vibration shifts upon deutration. *Journal of Molecular Graphics and Modelling*, 107:107976. https://doi.org/10.1016/j.jmgm.2021.107976

Ebraheem, H.A. (2013): Synthesis of some pyrimidine-2-one and pyrimidine-2-thione compounds. *Rafidain J. Sci*. 24(1):120-127. https://doi.org/10.33899/rjs.2013.67577

Frisch, A., Nelson, A.B. and Holder, A.J. (2000): *GAUSSVIEW User Manual*, Gaussian Inc, Pittsburgh, Pa, USA, 2000.

Gauss, J. (1992): Calculation of NMR chemical shifts at second-order many-body perturbation theory using gauge-including atomic orbitals. Chemical Physics Letters 191(6):614-620 https://doi.org/10.1016/0009-2614(92)85598-5

Hart, H., Craine, L.E., Hart, D.J. and Vinod T.K. (2012): Organic Chemistry (A short course). 13th Edition, Houghton-Mifflin, Boston. pp 68-81.

Isambert, N. and Lavilla, R. (2008): Heterocycles as key substrates in multicomponent reactions: the fast lane towards molecular complexity. *Chemistry*, 14(28):8444-54. https://doi.org/10.1002/chem.200800473 PMID: 18576454

Jamroz, M.E. and Jamróz, M.H. (2004): Vibrational energy distribution analysis, VEDA 4 Program, Warsaw, Poland, 2004.

Kanagathara, N., Thanigaiarasu, V.J., Sabari, V. and Elangovan, S. (2022): Density functional theoretical computational studies on 3-methyl 2-vinyl pyridinium phosphate. *Advances in Condensed Matter Physics*, volume 2022, Article ID 6488234 https://doi.org/10.1155/2022/6488234

Korkmaz, A., Rhyman, L. and Ramasami, P. (2023): Synthesis, characterization, DFT and molecular docking studies of acetone O-((2,5-dichlorophenyl)sulfonyl) oxime. *Physical Sciences Reviews*, 8(11):4017-4028. https://doi.org/10.1515/psr-2021-0230

Koroleva, E.V., Gusak, K.N. and Ignatovich, Z.V. (2010): Synthesis and applications of 2-aminopyrimidine derivatives as key intermediates in chemical synthesis of biomolecules. *Russian Chemical Reviews*, 79(8):655-682. https://doi.org/10.1070/rc2010v079n08abeh004116

Kumar, S. and Narasimhan, B. (2018): Therapeutic potential of heterocyclic pyrimidine scaffolds. *Chemistry Central Journal*, **(**12**):** 38. https://doi.org/10.1186/s13065-018-0406-5

Lagoja, I.M. (2005): Pyrimidine as constituent of natural biologically active compounds. *Chemistry and Biodiversity*, 2(1): 1 – 50. https://doi.org/10.1002/cbdv.200490173. PMID

Matsuzawa, N.N., Ishitani, A., Dixon, D.A. and Uda, T (2001): Time-dependent density functional theory calculations of photoabsorption spectra in the vacuum ultraviolet region. *J. Phys. Chem. A.* 105:4953-4962. https://bit.ly/3cyCabj

Mennucci, B., Tomasi, J., Cammi, R., Cheeseman, J.R., Frisch, M.J., Devlin, F.J., Gabriel, S. and Stephens, P.J. (2002): Polarizable continuum model (PCM) calculations of solvent effects on optical rotations of chiral molecules. *J. Phys. Chem. A.* 106(25):6102–6113.

Pallicer, J.M., Rosés, M., Ràfols, C., Bosch, E., and Pascual, R. (2014): Evaluation of log Po/w values of drugs from some molecular structure calculation software. ADMET & DMPK, 2(2):107-114. https://doi.org/10.5599/admet.2.2.45

Pasha, T.Y., Udupi, R.H. and Bhat, A.R. (2005): Synthesis and antimicrobial screening of some pyrimidine derivatives. *Indian Journal of Heterocyclic Chemistry*, 15:149-152.

Rao, N.S., Kistareddy, C., Balram, B. and Ram, B. (2012): Synthesis and antibacterial activity of novel imidazo[1,2-a]pyrimidine and imidazo[1,2-a]pyridine chalcones derivatives. *Der Pharma Chemica*, 4(6):2408-2415. www.derpharmachemica.com

Remington, J.R. (2005): The Science and Practice of Pharmacy, 21st Edition , Vol. II Ed D. B. Troy, pp 7-8.

Sharma. V. and Sharma, K.V. (2011): Synthesis and biological activity of some 2-amino-4,6-substituted-diarylpyrimidines: reactions of substituted chalcones with guanidinium carbonate. *RASAYAN J. Chem.* 4(1):17-23

Sudha, S., Anbuselvi, S.J., Thiruppathi, A., Vijayakumar, B., Kartikeya, P., Puthilibai, G. and Leevesh, K. (2022): Synthesis, structural, spectroscopic, and hirshfeld surface analysis, and DFT investigation of benzaldehyde semicarbazone. *Advances in Materials Science and Engineering*, Volume 2022 Article ID 4091119. https://doi.org/10.1155/2022/4091119

Umar, Y. and Abdalla, S. (2017): DFT Study of the molecular structure, conformational preference, HOMO, LUMO, and vibrational analysis of 2-, and 3-Furoyl Chloride. *J. Solution Chem.* 46:741-758. https://doi.org/10.1007/s10953-017-0601-3

Umar, Y., Cemal, P., Manirul, H.S.K., Sreekumar, P.A., Omar, A. and Ramasami, P. (2021): A comparative DFT study of tetracyanoquinodimethane and its Difluoro and Tetrafluoro Analogs. *Journal of the Indian Chemical Society*, 98(3):100032. https://doi.org/10.1016/j.jics.2021.100032

Vachala. S.D., Bhargavi, B. and Keloth, K.S. (2012): Fused pyrimidines: The heterocycle of diverse biological and pharmacological significance. *Der Pharma Chemica*, 4(1):255-265. http://derpharmachemica.com/archive

Waring, M. (2010): Lipophilicity in drug discovery. Expert Opinion on Drug Discovery, 5:235 - 248. https://doi.org/10.1517/17460441003605098

World Health Organization (WHO) (2021): Antimicrobial resistance. https://ahpsr.who.int/publications/i/item/global-action-plan-on-antimicrobial-resistance